



ELSEVIER

Contents lists available at ScienceDirect

MethodsX

journal homepage: [www.elsevier.com/locate/mex](http://www.elsevier.com/locate/mex)

## Method Article

# A high throughput Rb-Sr dating method using solution tandem ICP-MS/MS ( $^{87}\text{Sr}/^{86}\text{Sr}$ ) and standard addition calibration ICP-MS (Rb/Sr)



Christiaan T. Laureijs\*, Laurence A. Coogan, Jody Spence

*School of Earth and Ocean Science, University of Victoria, 3800 Finnerty Road, Victoria, British Columbia V8P 5C2, Canada*

## A B S T R A C T

Routine generation of large Rb-Sr age datasets has been limited by the time-consuming requirement of chromatographic isolation of Sr from Rb to avoid the isobaric interference of  $^{87}\text{Rb}^+$  on  $^{87}\text{Sr}^+$ . Recently, direct measurement of interference-free  $^{87}\text{Sr}/^{86}\text{Sr}$  has become possible with the advent of tandem quadrupole inductively coupled plasma mass spectrometry (ICP-MS/MS). Here, we describe a method that uses ICP-MS/MS to measure  $^{87}\text{Sr}/^{86}\text{Sr}$  combined with a standard addition calibration for precise determination of Rb/Sr, allowing efficient generation of Rb-Sr ages. The method is demonstrated on a suite of ~50 to 90 Myrs (million years) old celadonite samples that are dated with age uncertainties typically of  $\pm 2$  to 5 Myrs provided the sample Rb/Sr is  $> 2$ . A method to separate the phyllosilicate fraction from the bulk sample, because it commonly has a higher Rb/Sr more suitable for dating, using differential settling is also described.

- Differential settling allows high Rb/Sr phyllosilicates to be separated from other phases
- ICP-MS/MS allows  $^{87}\text{Sr}/^{86}\text{Sr}$  measurement without chromatographic isolation of  $\text{Sr}^+$  from  $\text{Rb}^+$
- Single-spike standard addition ICP-MS was used for Rb/Sr measurement

© 2021 The Author(s). Published by Elsevier B.V.

This is an open access article under the CC BY-NC-ND license (<http://creativecommons.org/licenses/by-nc-nd/4.0/>)

## A R T I C L E I N F O

*Method name:* Rb-Sr dating*Keywords:* Rb-Sr dating, Standard addition ICP-MS, ICP-MS/MS*Article history:* Received 21 December 2020; Accepted 9 March 2021; Available online 16 March 2021DOI of original article: [10.1016/j.chemgeo.2020.119995](https://doi.org/10.1016/j.chemgeo.2020.119995)

\* Corresponding author.

*E-mail address:* [laureijs@uvic.ca](mailto:laureijs@uvic.ca) (C.T. Laureijs).<https://doi.org/10.1016/j.mex.2021.101309>2215-0161/© 2021 The Author(s). Published by Elsevier B.V. This is an open access article under the CC BY-NC-ND license (<http://creativecommons.org/licenses/by-nc-nd/4.0/>)

## Specification table

Subject Area:	Earth and Planetary Sciences
More specific subject area:	<i>Geochronology</i>
Method name:	<i>Rb-Sr dating</i>
Name and reference of original method:	<ul style="list-style-type: none"> <li>• <i>Online separation of <math>^{87}\text{Sr}^+</math> from <math>^{87}\text{Rb}^+</math> through tandem ICP-MS/MS [2,3]</i></li> <li>• <i>Single-spike solution standard addition calibration ICP-MS [4]</i></li> </ul>

## Method details

### Method overview

Detailed resolution of many geological processes depend on the generation of large geochronology datasets. While high-throughput approaches have existed for some geochronometers for some time (e.g., laser-ablation U-Pb dating of zircons), until recently, Rb-Sr dating has been limited by relatively low throughput. This is due to the isobaric overlap of  $^{87}\text{Rb}^+$  and  $^{87}\text{Sr}^+$  on mass to charge ratio ( $m/z$ ) of 87 that requires chromatographic isolation of these elements prior to analysis (e.g. [5,6]). Developments in tandem quadrupole inductively coupled mass spectrometry (ICP-MS/MS) have recently made it possible to eliminate the chromatography step and directly measure  $^{87}\text{Sr}^+$  with online separation from  $^{87}\text{Rb}^+$  [2,3,10–12].

Tandem quadrupole mass spectrometry is based on two quadrupole mass filters (Q1 and Q2) bracketing a collision/reaction chamber [10,11]. The first quadrupole allows only a subset of species with a specific  $m/z$  to enter the collision/reaction chamber. The collision/reaction cell can then be used to either eliminate interferences or, as is the case here, to react with the species of interest generating a molecule with a different mass (mass shifted). In this case the second quadrupole (Q2) then focuses the mass-shifted species to the detector and, provided no other species allowed through Q1 undergo the same mass shift, the signal is now interference free.

Here we describe an approach to high-throughput Rb-Sr geochronometry using ICP-MS/MS for  $^{87}\text{Sr}/^{86}\text{Sr}$  isotopic analysis in combination with high-precision Rb/Sr ICP-MS analysis via standard addition. We use a dataset of 69 high Rb/Sr samples (celadonite,  $[\text{K}(\text{Fe}^{2+}, \text{Mg}^{2+})(\text{Fe}^{3+}, \text{Al}^{3+})\text{Si}_4\text{O}_{10}(\text{OH})_4]$ ) from the lava section of the Troodos ophiolite discussed in the co-submitted paper [1] as an example of this approach. An initial multi-element analysis was used to pre-screen the samples for suitability for Rb-Sr dating (i.e., having a sufficiently high Rb/Sr). A method for purification of a phyllosilicate fraction from bulk samples with low Rb/Sr, via differential settling in 18.2 M $\Omega$ -cm deionized water (DI), is also described.

### Sample preparation and digestion

Sample chips with <1 mm grain size were picked from crushed hand-samples and ground to a powder using an agate mortar and pestle. These samples, along with standards and blanks were dissolved following standard procedures for rock dissolution using Anachemia Environmental Grade HF and HNO<sub>3</sub> and DI. Around 50 mg of sample powder was weighed into a Teflon vial, then 2.5 mL HF (49%, 29 M) and 0.25 mL of HNO<sub>3</sub> (70%, 16 M) were added. Samples were sealed and placed on a hotplate for at least 24 h at ~120 °C. Lids were removed and the acids evaporated off by placing the vials on a hot plate at ~150 °C. When the samples reached a gel-like state, just before complete dryness, 2 mL of 8 M HNO<sub>3</sub> was added, the lids replaced, and the samples returned to the hotplate at ~120 °C for ~24 h. This acid was again evaporated to near complete dryness then 2 mL of 8 M HNO<sub>3</sub> was added. After leaving this on the hotplate overnight at ~80 °C the samples were transferred to clean HDPE bottles and diluted to produce a 0.32 M solution with a dilution factor of ~1000 by weight. Along with the celadonite samples the high Rb/Sr mineral standards NBS SRM 607 (K-feldspar) and CRPG Mica-Mg (phlogopite) were included as data quality checks. The following reference materials were included for major and trace element calibration, from the United States Geological Survey (USGS): BIR-1a (basalt powder), DNC-1 (dolerite powder), BHVO-2 (basalt powder); and from the Geological Survey of Japan (GSJ): JB-2 (basalt powder) and JP-1 (peridotite powder).

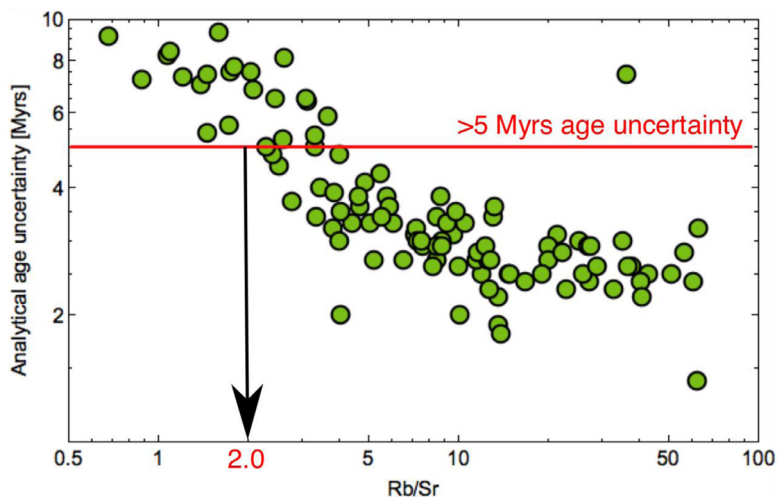


**Fig. 1.** The measured Rb/Sr from a routine multi-element analysis versus the final sample age uncertainty plotted on a logarithmic scale. The data shows that for this sample suite the age uncertainty begins to increase significantly as the Rb/Sr drops below  $\sim 5$  and only samples with Rb/Sr  $> 2$  are good targets for obtaining ages with uncertainties  $< 5$  Myrs (million years). The details for other samples suites will depend on both the analytical precision and accuracy as well as the sample ages.

#### *Purification of a fine-grained phyllosilicate fraction*

Low-temperature micas, and similar phyllosilicates, commonly have high Rb/Sr making them good targets for Rb/Sr dating. They also tend to be intimately intergrown with other phases that have lower Rb/Sr making separation by hand-picking challenging. Samples identified as impure celadonite (here based on a Rb/Sr  $< 2$ ; Fig. 1) were purified by differential settling in DI and the higher purity separate was re-digested. This process involved weighing 0.1 g of finely powdered sample into a metal-free 50 mL centrifuge tube. These tubes were then filled with 35 mL DI water, capped, shaken and left standing for the higher settling velocity material to settle out. After  $\sim 18$  h the high-density particles were observed to have settled to the bottom of the tube while the phyllosilicate fraction was still in suspension. The upper 30 mL of the cloudy solution containing suspended material was pipetted into a second, metal-free 50 mL centrifuge tube and centrifuged for 10 min to separate the suspended clay particles from the DI. After this the solution appeared clear with a small pellet of phyllosilicates visible at the bottom of the vial. The clear supernatant was pipetted off;  $\sim 10$  mL was retained for analysis and the remainder discarded. The pellet of separated phyllosilicate particles was re-suspended in  $\sim 3$  mL of DI, transferred into a Teflon vial and dried on a hot plate at  $\sim 80$  °C and then weighed. The recovered dry weights of the samples ranged from 5 to 20 mg. These separated samples were digested following the same procedure described above, but with the volume of reagents reduced. The first digestion step used 1.5 mL of 29 M HF and 0.15 mL of 16 M HNO<sub>3</sub> and the second digestion step used 1.2 mL 8 M HNO<sub>3</sub>. The final dilution factor of  $\sim 1000$  by weight was the same for as the bulk samples.

The 10 mL of supernatant DI retained from the settling experiments was acidified with 0.4 mL of 16 M HNO<sub>3</sub> and analyzed by multi-element analysis (described below). These solutions contained  $< 0.06$  ng Rb and  $< 0.7$  ng Sr, which is  $< 0.02$  and  $< 0.3\%$  respectively of the Rb and Sr contents of the samples, indicating that leaching of Rb and Sr during settling did not substantially change the sample composition. All of the separated clay samples had higher Rb/Sr than the corresponding bulk samples and for 11 out of 14 samples the Rb/Sr increased to  $> 2$  allowing them to be dated (e.g., Fig. 2).

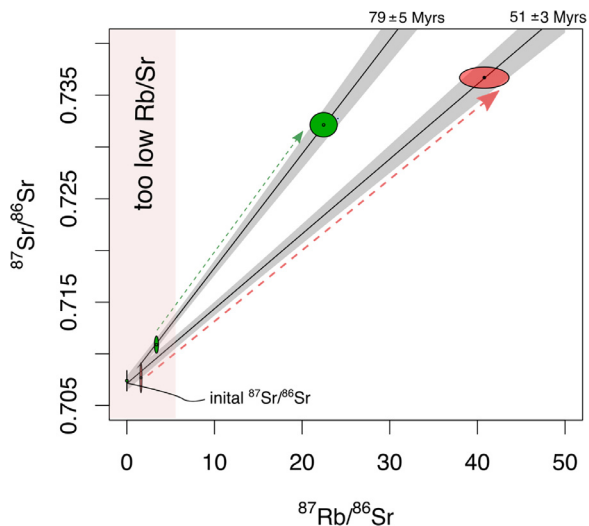


**Fig. 2.** Isochrons, generated with IsoplotR, showing both, data for an initial analysis (low Rb/Sr datapoints near the origin) and analysis of low settling velocity material that have much higher Rb/Sr for two samples CY2-117.8 (green) and 2017CL23 (red) with different ages. The  $^{87}\text{Rb}/^{86}\text{Sr}$  was obtained from the measured Rb/Sr ratios by assuming an abundance of  $^{87}\text{Rb}$  of 27.83% and an abundance of  $^{86}\text{Sr}$  of 9.86% corresponding to the natural abundances of these isotopes [19]. The grey uncertainty envelopes age uncertainties and error ellipses are all 95% confidence intervals. A fixed, initial  $^{87}\text{Sr}/^{86}\text{Sr}$  of  $0.7074 \pm 0.0002$  ( $1\sigma$ ; [16]) was assumed as discussed in the text. Purification by differential settling, as described in the text, increased the Rb/Sr ratio of the analyte (indicated by the coloured arrows) leading to much more precise age determinations than could have been achieved on the low Rb/Sr initial material. The red shaded area shows the region of samples with  $\text{Rb}/\text{Sr} < 2$  (and hence  $^{87}\text{Rb}/^{86}\text{Sr} < 5.6$ ) which produce low precision ages in our study [1] as shown in Fig. 1. (For interpretation of the references to color in this figure legend, the reader is referred to the web version of this article.)

### Analytical

All analyses were performed using an Agilent 8800 #100 ICP-MS/MS (also called a “Triple Quadrupole” ICP-MS) at the University of Victoria (Canada). This instrument was fitted with a concentric glass nebulizer, peltier cooled ( $2^\circ\text{C}$ ) Scott type double pass spray chamber, and nickel cones. The ICP-MS was tuned for optimal performance prior to each analytical session.

### Major- and trace-element analysis

Prior to Sr isotope and Rb/Sr analysis, a routine multi-element analysis was performed on all samples. Tuning followed standard procedure for ICP-MS analysis of digested rock solutions (no reaction cell gas, single quadrupole mode). This general analysis allows acquisition of a broad suite of trace element data and importantly gives an initial estimate of the Rb and Sr concentrations, to evaluate which samples are good targets for Rb-Sr dating, and which ones will require further purification. The samples were analyzed in blocks of 10 separated by a nitric acid blank (0.32 M) and a drift monitor solution made of a well-homogenized mixture of 10 randomly selected samples. Data processing followed the protocol described in [13], using Re as the internal standard. Secondary drift was approximated by a fourth-degree polynomial function for all analytes using data from the drift monitor solution. Calibration used the standards JP-1, BIR-1a, DNC-1, JB-2, W2a and BHVO-2 which were dissolved with the unknowns.

### Strontium Isotopic analysis by ICP-MS/MS

The basis of the ICP-MS/MS method for Sr-isotopic analysis is that the isobaric interference of  $^{87}\text{Rb}^+$  on  $^{87}\text{Sr}^+$  is removed by reaction of  $^{87}\text{Sr}^+$ , but not  $^{87}\text{Rb}^+$ , with a gas injected into the collision/reaction cell leading to the formation of Sr-molecules with an interference free mass (“mass-

**Table 1**

Acquisition parameters used for the Sr-isotope and standard addition analyses.

	Sr isotope Run (ICP-MS/MS)	Standard addition run
Analyte (Q1 $\rightarrow$ Q2)	Dwell times [s]	Dwell times [s]
$^{83}\text{Kr}^+$ (83 $\rightarrow$ 83)	0.001	
$^{102}\text{KrF}^+$ (83 $\rightarrow$ 102)	0.001	
$^{84}\text{SrF}^+$ (84 $\rightarrow$ 103)	0.3	
$^{85}\text{Rb}^+$ (85 $\rightarrow$ 85)	0.2	0.032
$^{104}\text{RbF}^+$ (85 $\rightarrow$ 104)	0.001	
$^{105}\text{SrF}^+$ (86 $\rightarrow$ 105)	0.3	
$^{106}\text{SrF}^+$ (87 $\rightarrow$ 106)	0.3	
$^{88}\text{SrF}^+$ (88 $\rightarrow$ 88)	0.01	0.032
$^{107}\text{SrF}^+$ (88 $\rightarrow$ 107)	0.3	
#Replicates	10	10
#Sweeps per replicate	100	25
Total acquisition time (s)	1443	18

shifted") which can then be measured [2,3,6,8,14]. In our study the ICP-MS/MS setup, tuning and analysis followed that described in [3].

The reaction cell gas (10% CH<sub>3</sub>F / 90% He, ultra-high purity, Praxair) was introduced to the reaction cell via the 4th cell gas channel set to 100% (~1 mL/min) and was allowed to equilibrate with the cell for ~ 24 h prior to tuning and analysis. The ICP-MS was run in MS/MS mode with the first quadrupole (Q1, before the cell) set to  $m/z = 87$  letting both  $^{87}\text{Sr}^+$  and  $^{87}\text{Rb}^+$  enter the cell. Within the cell Sr<sup>+</sup> reacts with CH<sub>3</sub>F generating  $^{106}\text{SrF}^+$ , a mass-shifted molecule, but Rb<sup>+</sup> does not. The second quadrupole (Q2, after the cell), set to  $m/z=106$ , allows an interference-free measurement of  $^{106}\text{SrF}^+$  as a proxy for  $^{87}\text{Sr}$ . The same approach was used for  $^{86}\text{Sr}$  and  $^{88}\text{Sr}$  to measure all Sr-isotopes as mass-shifted species. Acquisition details are given in Table 1. Importantly, there is no interference from Pd<sup>+</sup>, Ag<sup>+</sup> or Cd<sup>+</sup> as they are rejected at Q1. Confirmation that significant amounts of RbF<sup>+</sup> did not form was achieved by measuring the count rate for  $^{104}\text{RbF}^+$  which was always <15 counts per second (compared to >4500 counts per second for  $^{106}\text{SrF}^+$ ). Given the lower abundance of  $^{87}\text{Rb}$  than  $^{85}\text{Rb}$  this suggests <6 counts per second for  $^{106}\text{RbF}^+$  which is considered negligible. Interference from Kr<sup>+</sup> was monitored using  $^{83}\text{Kr}^+$  ( $m/z = 83$ ; <30 counts per second) and  $^{102}\text{KrF}^+$  ( $m/z = 102$ ; <1 count per second) and is also considered negligible.

The detector dead time was determined as part of each isotope run based on the measurement of the mass-shifted  $^{88}\text{Sr}/^{86}\text{Sr}$  ( $^{107}\text{SrF}^+ / ^{105}\text{SrF}^+$ ) count ratio from solutions containing 3, 10 and 30 ppb Sr. The measured dead time was found to match the manufacturer set dead time of  $28 \pm 0.23$  ns.

All Sr-isotopic analyses were performed using solutions containing 7 ppb Sr prepared in a class 1000 clean lab. This optimal concentration was selected after testing the precision of analytical runs at 1, 3, 7 and 10 ppb Sr. Precision is significantly degraded for solution concentrations <3 ppb Sr (Fig. 3) but some samples have low Sr contents and running these solutions at Sr concentrations higher than 7 ppb would lead to high matrix loads, potentially leading to decreased accuracy and precision. Samples were bracketed by analyses of the Sr-carbonate standard NIST SRM 987 also diluted to 7 ppb Sr in 0.32 M nitric acid.

Following the approach in [3], the dead time corrected count rate ratios for  $^{106}\text{SrF}^+ / ^{105}\text{SrF}^+$  ( $R^{106/105}$ ) and  $^{107}\text{SrF}^+ / ^{105}\text{SrF}^+$  ( $R^{107/105}$ ) were corrected for instrumental mass bias using a Russell law correction Eqs. (1) and (2). The Russell law is based on an exponential fractionation factor  $f$  (Eq. (1)), and was calculated using an  $^{88}\text{Sr}/^{86}\text{Sr}$  ratio of 8.375 [19]:

$$f = \ln \left[ \frac{8.375}{R^{107/105}} \right] / \ln \left[ \frac{M(^{88}\text{Sr})}{M(^{86}\text{Sr})} \right] \quad (1)$$

where  $M(^{88}\text{Sr})$  and  $M(^{86}\text{Sr})$  are the molar weights of  $^{88}\text{Sr}$  and  $^{86}\text{Sr}$ . The value of  $f$  for each analysis is then used to correct  $R^{106/105}$  for mass bias by the Russell-Law ( $R_{\text{Russell}}$ ; Eq. (2))

$$R_{\text{Russell}} = R^{106/105} \times \left( \frac{M(^{87}\text{Sr})}{M(^{86}\text{Sr})} \right)^f \quad (2)$$

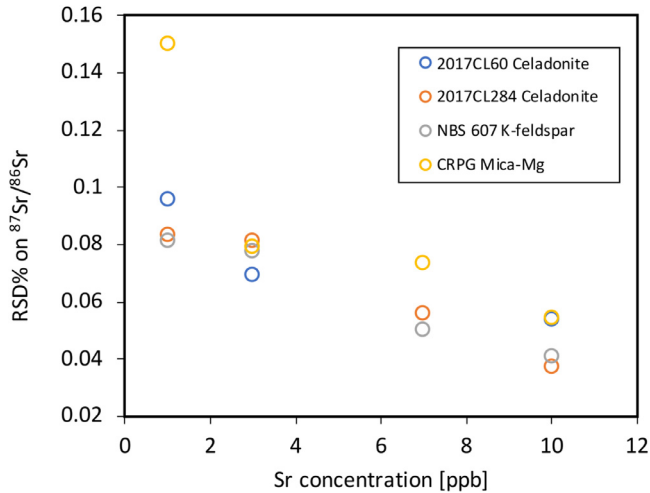


**Fig. 3.** Comparison of the percentage relative standard deviation (RSD%) of a Sr-isotope measurement with the Sr content of the analyte. This test was performed on four different solutions (two samples and two standards) and using four different solution Sr contents (1, 3, 7 and 10 ppb). The precision of the measured  $^{87}\text{Sr}/^{86}\text{Sr}$  ratio degrades at lower Sr concentrations. In the associated study [1], samples were measured at a Sr concentration of  $\sim 7$  ppb.

After Russell law correction, sample-standard bracketing was applied to correct for drift and to calibrate the  $R_{\text{Russell}}$  against the reference  $^{87}\text{Sr}/^{86}\text{Sr}$  ratio (0.71034; [15]) of the bracketing standard solution NIST SRM 987 ( $R_{\text{st.ref}}$ ):

$$R_{\text{SSB}} = \left( \frac{R_{\text{Russell}}}{(R_{\text{st}-1} + R_{\text{st}+1}) \times 0.5} \right) \times R_{\text{st.ref}} \quad (3)$$

The ratios  $R_{\text{st}-1}$  and  $R_{\text{st}+1}$  are measured Russell law corrected  $^{106}\text{SrF}^+ / ^{105}\text{SrF}^+$  ratios of the bracketing standard measurement before (subscript st-1) and after (subscript st+1) the sample. The  $^{87}\text{Sr}/^{86}\text{Sr}$  values obtained from Eq. 3 ( $R_{\text{SSB}}$ ) are the final sample  $^{87}\text{Sr}/^{86}\text{Sr}$ .

#### Sr and Rb measurement by standard addition calibration ICP-MS

Age determinations from Rb-Sr isochrons are just as sensitive to the precision and accuracy of the Rb/Sr concentration ratio as they are to the Sr-isotope ratio and a standard addition approach was used to determine this as follows. The samples were diluted in 0.32 M  $\text{HNO}_3$  to a dilution factor of  $\sim 30,000$  and a spike, containing sufficient Rb and Sr to increase the total Rb and Sr in the sample by at least a factor of three over the unspiked solution, was added to the split of each sample. The Rb and Sr concentrations measured during the initial multi-element analysis were used to guide the dilution factors and the amount and concentration of spike added. Because of the high dilution factors and hence low solution Rb and Sr concentrations (Rb 2.0 to 8.2 ppb and Sr 0.5 to 2.4 ppb) all sample handling as part of the dilution procedure was undertaken in a class 1000 clean lab.

For the Rb/Sr standard addition analytical run, the instrument was tuned to ensure maximum signal stability while keeping the sensitivity low enough that the detector remained in pulse counting mode. Analytes were measured “on mass” (Table 1). The Rb content of the standards NBS 607 K-feldspar and CRPG Mica-Mg were too high for both unspiked and spiked samples to be measured in pulse mode. Thus, in order to cross-check the data from pulse counting and analogue modes, we also analyzed the low Rb, high Sr, standards W2-a and BHVO-2 by standard addition (Table 2).

The samples were run in duplicate, with the spiked sample analysed twice bracketed with three analyses of the unspiked sample (i.e., a sequence of unspiked, spiked, unspiked, spiked, unspiked) following [4]. This approach allows drift to be monitored and accounted for [4]. The sample

**Table 2**

Measured (*m*) and reference (*ref*) values Rb and Sr concentrations and  $^{87}\text{Sr}/^{86}\text{Sr}$  ratio of rock and mineral standards used in this study. Ages of the NBS607 K-feldspar and CRPG Mica-Mg were determined here from two-point isochrons as described in the text with initial Sr-isotope ratios noted in the footnotes in . Reference values are the recommended from the GeoReM database [15] and compiled references therein except if indicated otherwise. Uncertainties are  $\pm 2\sigma$  on concentrations and ratios and 95% confidence intervals on the ages in million years (Myrs).

	BHVO-2		W2-a		NBS 607 K-feldspar		CRPG Mica-Mg	
	<i>m</i>	<i>ref</i>	<i>m</i>	<i>ref</i>	<i>m</i>	<i>ref</i>	<i>m</i>	<i>ref</i>
<b>Age [Myrs]</b>					1400 $\pm 22^b$	1418 $\pm 7.8$ [20]	528 $\pm 9.37^c$	519.4 $\pm 6.5$ [8]
<b>Rb [ppm]</b>	9.00 $\pm 0.02$	9.26 $\pm 0.09$	19.6 $\pm 0.05$	20.16 $\pm 1.57$	522.0 $\pm 4.4$	523.9 $\pm 0.3$	1320 $\pm 33$	1300 $\pm 114$
<b>Sr [ppm]</b>	401.3 $\pm 17.1$	394.1 $\pm 1.7$	186.8 $\pm 4.5$	195.4 $\pm 1.60$	64.6 $\pm 0.2$	65.0 $\pm 1$	26.9 $\pm 1$	27 $\pm 7$
<b><math>^{87}\text{Sr}/^{86}\text{Sr}</math></b>					1.2013 $\pm 0.0009$	1.2004 $\pm 0.0002^a$	1.8628 $\pm 0.0049$	1.8525 $\pm 0.0024^b$

<sup>a</sup> certified value by NIST;

<sup>b</sup> two-point isochron age with initial  $^{87}\text{Sr}/^{86}\text{Sr} = 0.71$  (no uncertainty assumed) from [20,21];

<sup>c</sup> two-point isochron age with initial  $^{87}\text{Sr}/^{86}\text{Sr} = 0.72607 \pm 0.00070$  from [8].

concentration was then calculated as follows:

$$C_{\text{Sample}} = \frac{C_{\text{spike}} \times \bar{I}_{\text{unspiked}}}{(I_{\text{spike}} - \bar{I}_{\text{unspiked}})} \times \text{DF} \quad (4)$$

Where  $C_{\text{spike}}$  is the known concentration (ppm) of either Rb or Sr that was added to the spiked sample solution,  $I_{\text{spike}}$  is the measured blank-corrected counts per second of the spiked unknown and  $\bar{I}_{\text{unspiked}}$  the average, blank-corrected counts per second of the two unspiked brackets in counts per second. The calculated concentration in the unspiked sample solution was then multiplied by the total dilution factor (DF) to obtain the sample concentrations of Rb and Sr. The two determinations of the sample Rb and Sr concentrations were averaged to produce the final data.

#### Method validation

##### Data quality

Raw count data for each individual Sr-isotopic analysis was collected as 10 “blocks” each made up of the average of 100 sweeps through the mass range (Table 1). The average count rate data is taken as the average of these 10 blocks and the standard error of these was used to calculate an analytical precision on the measured Sr-isotope ratio. The precision calculated this way for the  $^{87}\text{Sr}/^{86}\text{Sr}$  measured in [1] ( $N = 69$ ; Supplementary Table S1 of that study) ranges from  $\pm 0.012$  to 0.145% relative standard error (%RSE). Total procedural duplicates (i.e., starting from different splits of the same sample power and including separate digestions) agree within  $\pm 0.11\%$  RSE suggesting that the samples are reasonably homogeneous. The measured  $^{87}\text{Sr}/^{86}\text{Sr}$  are all within uncertainty of the reference values (Table 2) except the measured  $^{87}\text{Sr}/^{86}\text{Sr}$  of CRPG Mica-Mg, which differs from the reference value from [8] by 0.6%, which may reflect heterogeneity in this standard.

The standard error of the count rates  $I_{\text{unspiked}}$  and  $I_{\text{spiked}}$  in Eq. (4) was obtained from analysis blocks composed of 10 consecutive replicate measurements with 25 mass sweeps (Table 1). These count rate uncertainties were then propagated through Eq. (4) and taking the average of two determinations ( $C_{\text{sample}}$ ) of the Rb and Sr concentrations measured for each sample to obtain the precision of the final Rb and Sr concentrations measurements of a sample. The precision of the Rb and Sr concentration measurements were between  $\pm 0.13$  and 1.70 and  $\pm 0.03$  to 2.63% RSE, respectively. The resulting Rb/Sr have precisions of  $\pm 0.13$  to 2.81% RSE. Uncertainties due to weighing during spike preparation and sample spiking are estimated to be roughly  $\pm 0.0001$  g and thus contribute  $< 0.02\%$  to the total uncertainty of the measured Rb/Sr ratio; i.e., this is a negligible source of uncertainty. Based on seven replicate analyses of a single solution of a celadonite sample ( $\text{Rb/Sr} = 35.33 \pm 1.66$ ) the repeatability was  $\pm 0.6$  and 1.2% RSE for Rb and Sr respectively, and  $\pm 0.3\%$  RSE for Rb/Sr. This is within the analytical uncertainty estimated from counting statistics demonstrating the appropriateness of using counting statistic to estimate the uncertainties in this case. Total procedural duplicates, that include digestion of different aliquots of the same sample powder, had a relative difference in Rb/Sr of less than  $\pm 1.2\%$  which reflects both sample heterogeneity and analytical uncertainty.

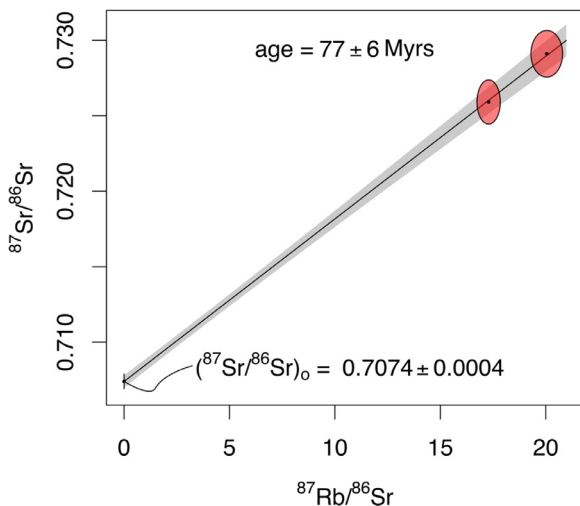


**Fig. 4.** Example of an isochron, produced with IsoplotR [17], based on two aliquots of the same sample (2017CL11). The initial  $^{87}\text{Sr}/^{86}\text{Sr}$  ratio is fixed at  $0.7074 \pm 0.0004$  [16]. The  $^{87}\text{Rb}/^{86}\text{Sr}$  was obtained from the measured Rb/Sr ratios by assuming an abundance of  $^{87}\text{Rb}$  of 27.83% and an abundance of  $^{86}\text{Sr}$  of 9.86% corresponding to the natural abundances of these isotopes [19]. Uncertainties are 95% confidence limits (ellipses and age uncertainty). The isochron plot demonstrates that heterogeneities between different aliquots of the same sample in Rb/Sr and  $^{87}\text{Sr}/^{86}\text{Sr}$  are not due to analytical uncertainties but natural compositional variation.

The Rb and Sr concentrations measured for the standards were within uncertainty of the reference values (Table 2) with the exception of the Rb content of BHVO-2 (measured =  $9.00 \pm 0.02$  ppm; reference =  $9.26 \pm 0.09$  ppm) and the Sr content of W2 (measured =  $186.8 \pm 4.5$  ppm; reference =  $195.4 \pm 1.6$  ppm). As discussed above, the spike for Sr was too small for accurate analyses of this Sr-rich standard. This shows the importance of using a large enough spike to obtain precise measurements by standard addition [4]. Including a series of multiple spikes for these standard additions, that covered a larger concentration range, could potentially improve the accuracy of the Rb and Sr concentration measurement. However, this would also lead to longer analysis times decreasing sample throughput and increasing the likelihood of instrumental drift, potentially degrading the precision of the measured Sr and Rb concentrations [4].

#### Rb-Sr ages

Sample ages were determined using two-point Rb-Sr isochrons using the measured Rb/Sr and  $^{87}\text{Sr}/^{86}\text{Sr}$  ratios and an estimate of the initial  $^{87}\text{Sr}/^{86}\text{Sr}$ . The latter comes from the average  $^{87}\text{Sr}/^{86}\text{Sr}$  of cogenetic calcite [16] that are found alongside the celadonite samples. Calcite has a very low Rb/Sr and thus its  $^{87}\text{Sr}/^{86}\text{Sr}$  is almost identical to the initial ratio justifying its use to define the initial  $^{87}\text{Sr}/^{86}\text{Sr}$ . Isochron age uncertainties were calculated using maximum likelihood regressions [22] implemented in the online version of IsoplotR ([17]; <https://www.ucl.ac.uk/~ucfbpve/isoplotr/home/index.html>). The age uncertainties including propagation of the uncertainty of the decay constant  $\lambda_{\text{Rb-Sr}}$  ( $1.3972 \pm 0.0045$ ; [18]). The Rb/Sr are high enough that the contribution of the uncertainty of the initial  $^{87}\text{Sr}/^{86}\text{Sr}$  on the age is negligible. For the age range of the dataset, from 43 to 92 Myrs, an average age uncertainty of around  $\pm 5$  Myrs (million years, 90% confidence limit) is obtained.

To test both sample age homogeneity, and the analytical approach, for some samples multiple celadonite aliquots were picked. These plot on a common isochron despite having variable Rb/Sr and  $^{87}\text{Sr}/^{86}\text{Sr}$  (Fig. 4). This variability in composition is not unexpected for such hydrothermal minerals, especially given that perfectly pure materials could not be separated, and suggests that individual samples grew over a relatively short time period. In addition, two-point isochron ages calculated for the NBS SRM607 K-feldspar and CRPG Mica-Mg agree with published Rb-Sr ages (Table 2). Hence,



two-point Rb-Sr isochron ages seem to give reliable estimates of crystallization ages. Although the Rb-Sr age uncertainties measured here are larger than those achievable using more expensive, and more time consuming, higher-precision methods (e.g., TIMS or MC-ICP-MS; e.g., [20]), the method presented here is faster, allowing the generation of large age datasets.

## Conclusions

We outlined a method to date phyllosilicates efficiently by combining direct measurement of  $^{87}\text{Sr}/^{86}\text{Sr}$  ratios from ICP-MS/MS with standard addition calibration ICP-MS for Rb/Sr ratios. The method eliminates the need for chromatographic isolation of  $^{87}\text{Sr}$  and thus increases significantly the sample throughput helping facilitate the production of large geochronological datasets. Ages and Rb/Sr ratios of internationally recognized standards were reproduced with Rb-Sr age uncertainties typically between  $\pm 2$  and 5 Myr (90% confidence). Low Rb/Sr ratios limit the accuracy and precision of this method. Physical separation of high Rb/Sr phyllosilicates via differential settling in DI was used to increase the number of samples with high Rb/Sr. An alternative strategy for analysis of just high Rb/Sr material is laser ablation ICP-MS/MS [2,7–9]. The ages obtained reflect real geological ages as multiple picked aliquots of the same sample plot on a common isochron.

## Declaration of Competing Interest

The authors declare that they have no competing financial interests or personal relationships that could have appeared to influence the work reported in this paper.

## Acknowledgment

We thank the editor Régis Braucher and two anonymous reviewers for their valuable suggestions that significantly improved the manuscript. Thanks also go to Hollie Johnson and Erinn Raftery for assistance with sample preparation.

## References

- [1] C.T. Laureijs, L.A. Coogan, J. Spence, Regionally variable timing and duration of celadonite formation in the Troodos lavas (Cyprus) from Rb-Sr age distributions, *Chem. Geol.* 560 (2021) 119995, doi:[10.1016/j.chemgeo.2020.119995](https://doi.org/10.1016/j.chemgeo.2020.119995).
- [2] T. Zack, K.J. Hogmalm, Laser ablation Rb/Sr dating by online chemical separation of Rb and Sr in an oxygen-filled reaction cell, *Chem. Geol.* 437 (2016) 120–133, doi:[10.1016/j.chemgeo.2016.05.027](https://doi.org/10.1016/j.chemgeo.2016.05.027).
- [3] E. Bolea-Fernandez, L. Balcaen, M. Resano, F. Vanhaecke, Tandem ICP-mass spectrometry for Sr isotopic analysis without prior Rb/Sr separation, *J. Anal. At. Spectrom.* 31 (2016) 303–310, doi:[10.1039/C5JA00157A](https://doi.org/10.1039/C5JA00157A).
- [4] P. Abbyad, J. Tromp, J. Lam, E. Salin, Optimization of the technique of standard additions for inductively coupled plasma mass spectrometry, *J. Anal. At. Spectrom.* 16 (2001) 464–469, doi:[10.1039/b100672j](https://doi.org/10.1039/b100672j).
- [5] C. Pin, C. Bassin, Evaluation of a strontium-specific extraction chromatographic method for isotopic analysis in geological materials, *Anal. Chim. Acta* 269 (1992) 249–255, doi:[10.1016/0003-2670\(92\)85409-Y](https://doi.org/10.1016/0003-2670(92)85409-Y).
- [6] L.J. Moens, F.F. Vanhaecke, D.R. Bandura, et al., Elimination of isobaric interferences in ICP-MS, using ion–molecule reaction chemistry: Rb/Sr age determination of magmatic rocks, a case study, *J. Anal. At. Spectrom.* 16 (2001) 991–994, doi:[10.1039/B103707M](https://doi.org/10.1039/B103707M).
- [7] E. Bolea-Fernandez, S.J.M. Van Malderen, L. Balcaen, et al., Laser ablation-tandem ICP-mass spectrometry (LA-ICP-MS/MS) for direct Sr isotopic analysis of solid samples with high Rb/Sr ratios, *J. Anal. At. Spectrom.* 31 (2016) 464–472, doi:[10.1039/C5JA00404G](https://doi.org/10.1039/C5JA00404G).
- [8] K.J. Hogmalm, T. Zack, A.K.O. Karlsson, et al., *In situ* Rb–Sr and K–Ca dating by LA-ICP-MS/MS: an evaluation of  $\text{N}_2\text{O}$  and  $\text{SF}_6$  as reaction gases, *J. Anal. At. Spectrom.* 32 (2017) 305–313, doi:[10.1039/C6JA00362A](https://doi.org/10.1039/C6JA00362A).
- [9] M. Tillberg, H. Drake, T. Zack, et al., *In situ* Rb–Sr dating of slickenfibers in deep crystalline basement faults, *Sci. Rep.* 10 (2020) 562, doi:[10.1038/s41598-019-57262-5](https://doi.org/10.1038/s41598-019-57262-5).
- [10] E. Bolea-Fernandez, L. Balcaen, M. Resano, F. Vanhaecke, Overcoming spectral overlap via inductively coupled plasma-tandem mass spectrometry (ICP-MS/MS). A tutorial review, *J. Anal. At. Spectrom.* 32 (2017) 1660–1679, doi:[10.1039/C7JA00010C](https://doi.org/10.1039/C7JA00010C).
- [11] L. Balcaen, E. Bolea-Fernandez, M. Resano, F. Vanhaecke, Inductively coupled plasma – Tandem mass spectrometry (ICP-MS/MS): a powerful and universal tool for the interference-free determination of (ultra)trace elements – a tutorial review, *Anal. Chim. Acta* 894 (2015) 7–19, doi:[10.1016/j.aca.2015.08.053](https://doi.org/10.1016/j.aca.2015.08.053).
- [12] E. Bolea-Fernandez, L. Balcaen, M. Resano, F. Vanhaecke, Potential of methyl fluoride as a universal reaction gas to overcome spectral interference in the determination of ultratrace concentrations of metals in biofluids using inductively coupled plasma-tandem mass spectrometry, *Anal. Chem.* 86 (2014) 7969–7977, doi:[10.1021/ac502023h](https://doi.org/10.1021/ac502023h).

- [13] S.M. Eggins, J.D. Woodhead, L.P.J. Kinsley, et al., A simple method for the precise determination of  $\geq 40$  trace elements in geological samples by ICPMS using enriched isotope internal standardisation, *Chem. Geol.* 134 (1997) 311–326, doi:[10.1016/S0009-2541\(96\)00100-3](https://doi.org/10.1016/S0009-2541(96)00100-3).
- [14] F. Vanheacke, G. De Wannemacker, L. Balcaen, L. Moens, The use of dynamic cell ICP mass spectroscopy to facilitate Rb-Sr age determination, in: *Geochronology: Linking the Isotopic Record with Petrology and Textures*, Geological Society, London, 2003, pp. 173–181.
- [15] K.P. Jochum, U. Nohl, K. Herwig, et al., GeoReM: a new geochemical database for reference materials and isotopic standards, *Geostand. Geoanal. Res.* 29 (2005) 333–338, doi:[10.1111/j.1751-908X.2005.tb00904.x](https://doi.org/10.1111/j.1751-908X.2005.tb00904.x).
- [16] L.A. Coogan, S.E. Dosso, Alteration of ocean crust provides a strong temperature dependent feedback on the geological carbon cycle and is a primary driver of the Sr-isotopic composition of seawater, *Earth Planet. Sci. Lett.* 415 (2015) 38–46, doi:[10.1016/j.epsl.2015.01.027](https://doi.org/10.1016/j.epsl.2015.01.027).
- [17] P. Vermeesch, IsoplotR: a free and open toolbox for geochronology, *Geosci. Front.* 9 (2018) 1479–1493, doi:[10.1016/j.gsf.2018.04.001](https://doi.org/10.1016/j.gsf.2018.04.001).
- [18] I.M. Villa, P. De Bièvre, N.E. Holden, P.R. Renne, IUPAC-IUGS recommendation on the half-life of  $^{87}\text{Rb}$ , *Geochim. Cosmochim. Acta* 164 (2015) 382–385, doi:[10.1016/j.gca.2015.05.025](https://doi.org/10.1016/j.gca.2015.05.025).
- [19] K.J.R. Rosman, P.D.P. Taylor, Isotopic compositions of the elements 1997 (Technical Report), *Pure Appl. Chem.* 70 (1998) 217–235, doi:[10.1351/pac199870010217](https://doi.org/10.1351/pac199870010217).
- [20] O. Nebel, K. Mezger, Reassessment of the NBS SRM-607 K-feldspar as a high precision Rb/Sr and Sr isotope reference, *Chem. Geol.* 233 (2006) 337–345, doi:[10.1016/j.chemgeo.2006.03.003](https://doi.org/10.1016/j.chemgeo.2006.03.003).
- [21] Y. Amelin, A.N. Zaitsev, Precise geochronology of phoscorites and carbonatites, *Geochim. Cosmochim. Acta* 66 (2002) 2399–2419, doi:[10.1016/S0016-7037\(02\)00831-1](https://doi.org/10.1016/S0016-7037(02)00831-1).
- [22] Derek York, Norman Evensen, Margarita López Martínez, Joná De Basabe Delgado, et al., Unified equations for the slope, intercept, and standard errors of the best straight line, *American Journal of Physics* 72 (3) (2004) 367–375, doi:[10.1119/1.1632486](https://doi.org/10.1119/1.1632486).